Communication

A New Family of Ru Complexes for Water Oxidation

Ruifa Zong, and Randolph P. Thummel

J. Am. Chem. Soc., **2005**, 127 (37), 12802-12803• DOI: 10.1021/ja054791m • Publication Date (Web): 27 August 2005

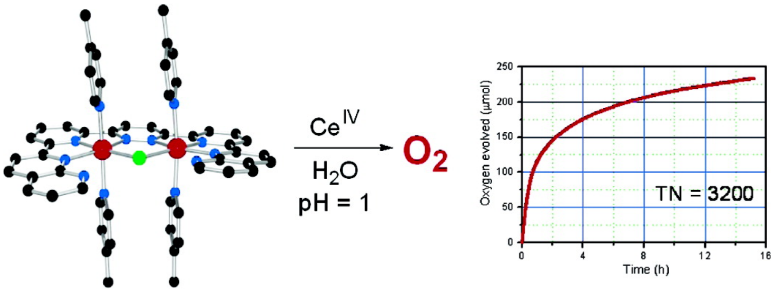

Journal of the American Chemical Society is published by the American Chemical Society. 1155 Sixteenth Street N.W., Washington, DC 20036

J|A|C|S
COMMUNICATIONS

A New Family of Ru Complexes for Water Oxidation

Ruifa Zong and Randolph P. Thummel*

Department of Chemistry, 136 Fleming Building, University of Houston, Houston, Texas 77204-5003

Received July 18, 2005; E-mail: thummel@uh.edu

Green plants have developed complex catalytic systems for the decomposition of water into its elements, and our understanding of these systems is pointing the way to the design of simpler catalysts. The oxygen-evolving catalyst (OEC) of photosystem II is a tetranuclear manganese cluster that uses a high oxidation state of the metal to promote the conversion of metal−aquo to metal−oxo species leading to dioxygen. Synthetic analogues of this OEC have been prepared which show modest catalytic activity toward water oxidation.[1] Ruthenium-based catalysts also show promise for water oxidation. One such system is the blue dimer *cis,cis*-$[\{Ru(bpy)_2(H_2O)\}_2O](ClO_4)_4$ (bpy = 2,2′-bipyridine) in which the two Ru fragments are linked by a μ-oxo bridge which is prone to cleavage, thus limiting the lifetime of the catalyst.[2] This problem has been addressed by the design of ligands that bridge the two metal centers and thus increase the stability of the catalyst.[3,4]

We have prepared a family of bis-tridentate ligands capable of holding two metals in well-defined orientations with respect to one another. One member of this family is 3,6-bis-[6′-(1″,8″-naphthyrid-2″-yl)-pyrid-2′-yl]pyridazine (**1**) which is prepared in several steps from 3,6-dichloropyridazine.[5] When treated with $[Ru(DMSO)_4Cl_2]$ in ethanol followed by excess 4-substituted pyridine in the presence of triethylamine, eight components assemble to form complexes **2a**−**c** as the only isolated product in yields of 44−56%. The diamagnetic Ru(II,II) complexes were characterized by their ^1H NMR spectra which showed well-resolved peaks for the protons of the equatorial ligand as well as two 8H AA′BB′ patterns for the axial pyridine protons. The structure of **2b** was further verified by mass spectroscopy and a preliminary X-ray analysis of its perchlorate salt (Figure S1). The Ru−Ru distance is approximately 3.7 Å, in good agreement with other Ru_2 catalysts.[2,4] The μ-Cl bridge is quite stable, and the chloride cannot be displaced even upon exposure to Ag^+ in refluxing acetone.

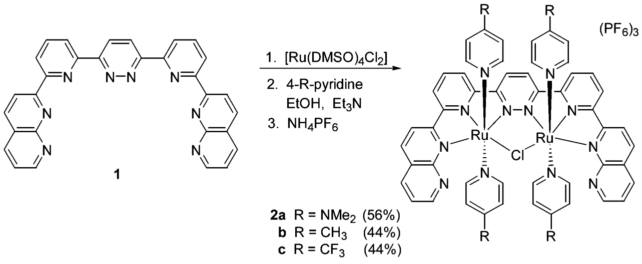

To evaluate the importance of the dinuclear arrangement of **2a**−**c**, we also prepared their mononuclear analogues. The Friedländer condensation of 2-aminonicotinaldehyde with 4-*tert*-butyl-2,6-diacetylpyridine in ethanolic KOH provided the ligand **5** in 87% yield.[6] The reaction of equimolar amounts of **5** and $RuCl_3{\cdot}3H_2O$ in ethanol afforded $[Ru(\mathbf{5})Cl_3]$ which is not isolated but rather treated directly with excess of a 4-substituted pyridine to afford the complexes **6a**−**c** in isolated yields of 19−59%. The structures of the complexes were established by their ^1H NMR spectra which showed coupling and shielding effects similar to the dinuclear system.

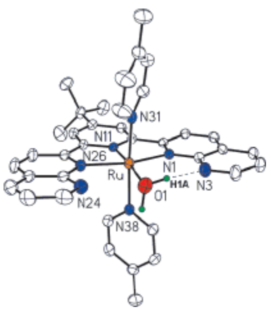

Figure 1. ORTEP plot of the cation of **6b**; hydrogens (except water) omitted for clarity.

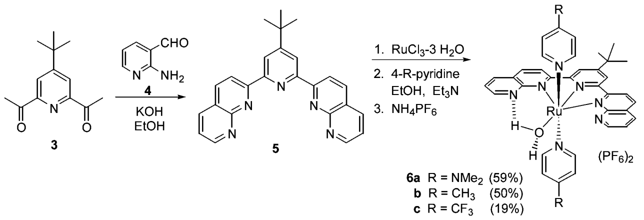

The *trans*-geometry for **6b** was confirmed by a single-crystal X-ray analysis, and an ORTEP plot of the cation is illustrated in Figure 1. The water molecule is positioned in the Ru-**5** plane with an Ru−O distance of 2.137(5) Å which is comparable to other Ru(II)−aquo polypyridine complexes.[7] The Ru−N distances fall within the normal range of 2.09−2.10 Å with the exception of Ru−N11 which is shorter (1.92 Å) as expected. The torsion angles about the pyridine-naphthyridine bonds are only about 1.5°, indicating that **5** is essentially planar in the complex. The water molecule is H-bonded to an uncomplexed naphthyridine nitrogen on one side only with an N3−H1A distance of about 2.27 Å and an O1−H1A−N3 angle of 122.4°. It is noteworthy that for this system, unlike **2b**, the chloro complex cannot be isolated and only the H-bonded aquo species is produced. H-bonding helps to stabilize the aquo complex as noted previously for a similar complex involving tpy (2,2′:6′,2″-terpyridine) and 2-pyridone.[8]

The electronic absorption data for the complexes are summarized in Table 1, and the long wavelength region of the absorption spectra of **6a**−**c** is illustrated in Figure 2. The lowest-energy electronic transition for such Ru(II) complexes is generally associated with a metal-to-ligand charge transfer (MLCT) state resulting from the promotion of an electron from a metal d-orbital to the π^*-orbital of the most electronegative ligand, in this case, **5**. Both the energy and intensity of this band are sensitive to the nature of the axial pyridine ligands. The σ-donor ability of the pyridine increases as the 4-substituent is varied from CF_3 to CH_3 to NMe_2, resulting in a consistent red-shift of the MLCT band from 577 to 669 nm. The shape of the band remains almost invariant, indicating that the effect

10.1021/ja054791m CCC: $30.25 © 2005 American Chemical Society

Table 1. Electron Absorption[a] and Cyclic Voltammetric[b] Data for **2a**−**c** and **6a**−**c**

complex	λ_{max} (ϵ)	$E_{1/2}^{Ox}$ (ΔE)	$E_{1/2}^{Red}$ (ΔE)
2a	208 (44620), 338 (44970), 504 (3980), 685 (5500)	0.92 (85), 1.16 (118)	−0.74 (77), −1.07 (86), −1.33 (99)
2b	208 (45320), 338 (45480), 505 (7280), 613 (8550)	1.25 (99), 1.66 (110)	−0.65 (72), −1.02 (76), −1.24 (82), −1.73 (81)
2c	208 (48290), 340 (43240), 380 (18950), 484 (10950), 571 (9830)	1.47 (127)	−0.54 (95), −0.94 (73), −1.13 (95)
6a	208 (44290), 325 (31220), 353 (24810), 562 (2230), 669 (3800)	0.91 (77)	−0.93 (98), −1.33 (116)
6b	208 (18760), 325 (16310), 350 (18580), 522 (2710), 618 (4280)	1.24 (89)	−0.87 (70), −1.26 (99)
6c	208 (39220), 324 (24560), 351(27300) 370 (26250), 499 (3550), 577 (4620)	1.39 (100)	−0.82 (82), −1.20 (96)

[a] Measured in acetone (5.0 × 10^{-5} M). [b] Measured with glassy carbon electrode at 100 mV/s in CH_3CN containing 0.1 M N(*n*-Bu)$_4$PF$_6$ and reported in volts relative to SCE; $E_{1/2} = (E_{pa} + E_{pc})/2$ in volts and $\Delta E = (E_{pa} - E_{pc})$ in mV.

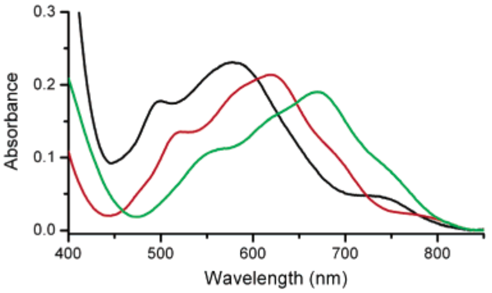

Figure 2. Visible spectra of **6a**−**c** recorded in acetone (5 × 10^{-5} M): **6a** (green), **6b** (red), **6c** (black).

Table 2. Water Oxidation Data for **2a**−**c** and **6a**−**c**

complex	TN[a]	κ (10^{-4} s^{-1})[b]	complex	TN[a]	κ (10^{-4} s^{-1})[b]
2a	210	5.6	**6a**	50	7.8
2b[c]	3200	7.7	**6b**	580	3.5
2c	100	1.4	**6c**	70	3.5

[a] TN = turnover number (moles of generated O_2 vs moles of catalyst). [b] κ = first-order rate constant. [c] Concentration reduced 10×.

involves predominantly the Ru(II) d-orbital, and the intensity of the band decreases as the pyridine becomes a better donor. For the dinuclear complexes, the MLCT band is somewhat broadened but follows the same general trend with variation of the axial ligand.

The electrochemical properties of **2a**−**c** and **6a**−**c** are summarized in Table 1 and vary in a fashion consistent with the electronic spectra. For the mononuclear complex **6a**, where acetonitrile replaces the bound water, the dimethylaminopyridine behaves as a strong donor and facilitates oxidation which occurs at a potential 0.48 V less positive than for **6c**, having a more electronegative trifluoromethylpyridine. The reductions are influenced in the same sense but to a lesser extent. The ability of the equatorial ligand to accept an electron is partly dependent on the donor ability of the axial ligand as transmitted through the complexed metal, making reduction easier for **6c**. The behavior of the dinuclear complexes follows the same trends, except that for **2a** and **2b** a second oxidation is observed, corresponding to formation of the Ru(III, III) species. The equatorial ligand **1** is expected to be a better acceptor than **5** and, hence, the more positive reductions.

The catalytic activity of **2a**−**c** and **6a**−**c** toward water oxidation was evaluated. In a typical run, an acetonitrile solution (0.10 mL) of the catalyst (0.01 M in Ru) was added to 3 mL of an aqueous Ce(IV)−CF_3SO_3H solution (pH = 1.0) at 24 °C. The generated oxygen was measured with an oxygen probe (YSI 5331) and monitor (YSI 5300). Fitting the evolved oxygen vs time curve gives the first-order rate constants reported in Table 2. At pH = 1, the dimethylamino group is protonated and thus behaves more as an electron acceptor than donor group. For both mono- and dinuclear complexes, the highest turnover numbers are observed with 4-methylpyridine as the axial ligand and these numbers indicate a robust catalyst as compared to other previously reported systems.[2−4] The mononuclear system **6a** produces only a small amount of dioxygen but does so at a fast rate. It is interesting that the mononuclear catalyst functions so well.[9] We also examined several other similar mononuclear Ru(II)−aquo systems such as $[Ru(tpy)(bpy)(H_2O)]^{2+}$ and $[Ru(tpy)(binap\text{-}n)(H_2O)]^{2+}$ (binap-*n* = 3,3′-polymethylene bridged-2,2′-bi[1,8]naphthyridine)[8] and found no evidence for O_2 formation, indicating that complexes **6a**−**c** are unique in this regard.

Future studies will look at the effect of structural changes in both the axial and equatorial ligands as well as mechanistic aspects of the oxidation. The ultimate goal in the design of a practical photocatalyst will be to drive the oxidation process with light, and this issue is under consideration.

Acknowledgment. We thank the Division of Chemical Sciences, Office of Basic Energy Sciences, U.S. Department of Energy (Contract No. DE-FG03-02ER15334) and the Robert A. Welch Foundation (E-621) for financial support of this work. We also thank Dr. James Korp for assistance with the X-ray analyses and Professor Jim Hurst for helpful advice.

Supporting Information Available: The synthetic details for **2a**−**c**, **5**, and **6a**−**c**; the X-ray crystallography for **2b** (Figure S1) and **6b** (CIF file); and a typical oxygen evolution curve (Figure S2). This material is available free of charge via the Internet at http://pubs.acs.org.

References

(1) (a) Limburg, J.; Vrettos, J. S.; Liable-Sands, L. M.; Rheingold, A. L.; Crabtree, R. H.; Brudvig, G. W. *Science* **1999**, *283*, 1524−1527. (b) Narita, M.; Narita, K. *J. Am. Chem. Soc.* **2004**, *126*, 8084−8085. (c) Shimazaki, Y.; Nagano, T.; Takesue, H.; Ye, B.-H.; Tani, F.; Naruta, Y. *Angew. Chem., Int. Ed.* **2004**, *43*, 98−100. (d) Rüttinger, W.; Dismukes, G. C. *Chem. Rev.* **1997**, *97*, 1−24.
(2) (a) Gersten, S. W.; Samuels, G. J.; Meyer, T. J. *J. Am. Chem. Soc.* **1982**, *104*, 4029−30. (b) Gilbert, J. A.; Eggleston, D. S.; Murphy, W. R., Jr.; Geselowitz, D. A.; Gersten, S. W.; Hodgson, D. J.; Meyer, T. J. *J. Am. Chem. Soc.* **1985**, *107*, 3855−3864.
(3) (a) Wada, T.; Tsuge, K.; Tanaka, K. *Angew. Chem., Int. Ed.* **2000**, *39*, 1479−1482. (b) Wada, T.; Tsuge, K.; Tanaka, K. *Inorg. Chem.* **2001**, *40*, 329−337.
(4) Sens, C.; Romero, I.; Rodriguez, M.; Llobet, A.; Parella, T.; Benet-Buchholz, J. *J. Am. Chem. Soc.* **2004**, *126*, 7798−7799.
(5) Zong, R.; Hammitt, R.; Wang, D.; Thummel, R. P. Manuscript in preparation.
(6) (a) Thummel, R. P.; Jahng, Y. *J. Org. Chem.* **1985**, *50*, 2407−2412. (b) Thummel, R. P. *Synlett* **1992**, 1−12.
(7) Zong, R.; Naud, F.; Segal, C.; Burke, J.; Wu, F.; Thummel, R. P. *Inorg. Chem.* **2004**, *43*, 6195−6202.
(8) Kelson, E. P.; Phengsy, P. P. *J. Chem. Soc., Dalton Trans.* **2000**, 4023−4024.
(9) Collin, J. P.; Sauvage, J. P. *Inorg. Chem.* **1986**, *25*, 135−41.

JA054791M